Acta of Bioengineering and Biomechanics
Vol. 17, No. 4, 2015

Original paper
DOI: 10.5277/ABB-00153-2014-04

Quasi-static and dynamic properties of the intervertebral disc: experimental study and model parameter determination for the porcine lumbar motion segment

ÂNGELO R.G. ARAÚJO*, NUNO PEIXINHO, ANTÓNIO C.M. PINHO, J.C.P. CLARO

University of Minho, Departamento de Engenharia Mecânica, Guimarães, Portugal.

Purpose: The study of axial loading is essential to determine the properties of intervertebral disc. The objectives of this work are (1) to quantify the mechanical properties of porcine lumbar intervertebral discs under static and cyclic compressive loading, and (2) to determine the parameters of a five-parameter rheological model for porcine and compare them with those obtained for human lumbar intervertebral discs. Methods: Thus, the porcine lumbar motion segments were subjected to quasi-static and dynamic compression tests. The quasi-static tests were used to obtain the static stiffness coefficient at different strain rates, while the data from the cyclic compressive tests were used to both determine the dynamic stiffness coefficient and to be fitted in a 5-parameter model, in order to simulate the creep response of the porcine intervertebral discs. Results: The results demonstrated that dynamic stiffness coefficient of porcine discs is between four and ten times higher than the static stiffness coefficient, depending on load applied. The parameters of the rheological model suggested a low permeability of nucleus and endplate during the fast response of porcine discs. In addition, the fast response in terms of displacement is four times higher than those documented for human discs. Conclusions: This study revealed that care must be taken on the comparison between porcine and human discs, since they present different behaviour under quasi-static and dynamic compressive loading.

Key words: *intervertebral disc, dynamic response, stiffness, axial compression, quasi-static response*

1. Introduction

The IVD is comprised by a peripheral angle-ply laminated ring, the annulus fibrosus – AF, with the gelatinous nucleus pulposus (NP) in its center, bounded by the cartilaginous endplate (CEP). This intricate and inhomogeneous IVD structure allows six degrees of freedom load-bearing movement, load transfer and energy dissipation to the spine [25].

The mechanical response of the disc to loading is time-dependent, presenting a complex behavior: while the short time response is governed by viscoelastic phenomena [9], the long term response is guided by osmotic events – the fluid flows through NP, AF and endplate, ruled by fixed proteoglycans charges [31].

During daily routine events, this structure is subjected to several ranges of loads, where the quasi-static and cyclic axial compressions are the predominant ones. Several studies showed that compressive loads are responsible for great oscillations on intradiscal pressure [31], disc height [18] and disc volume [24]. In terms of intradiscal pressure, an increase on the compressive load applied to healthy discs promotes an upturn on NP pressure [31]. Since the NP can be considered as incompressible, the AF bulges outward [33], which, together with osmotic phenomenon, lead to a loss on both disc height and volume. Thus, the disc hydration influences the disc mechanics, namely the stiffness and creep properties during axial loading [14], [25].

To assess the mechanical properties of the IVD, several samples of animal spines are widely used, namely the smallest functional unit of the spine, the motion segment – MS [19], [21], [25], [33] (Fig. 1). The animal disc samples are commonly used since

* Corresponding author: Ângelo R.G. Araújo, Departamento de Engenharia Mecânica, Campus de Azurém, 4800-058 Guimarães, Portugal. Tel: +35 1913578579, e-mail: angelo14araujo@gmail.com

Received: August 5th, 2014
Accepted for publication: January 15th, 2015

they present higher availability and lower cost when compared with human tissues. Among disc animal models, rat [21], goat [35], bovine [27] and porcine [29], [33] are widely used in both *in vivo* and *in vitro* studies. They can be prepared directly and gripped to perform MS studies and surgical techniques.

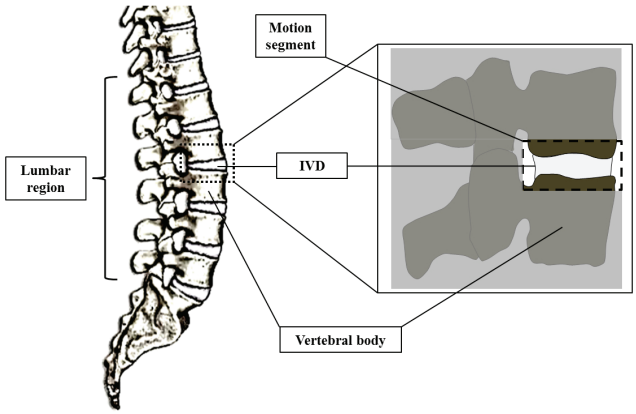

Fig. 1. A lumbar motion segment representation. The MS adopted for the study is composed by an IVD and half of both the adjacent vertebral bodies, without posterior elements. This structure is highlighted by the dashed rectangle

Although the common use of these animal models, data extrapolation from different animal tests to human IVD properties should be carefully done, since benchmark values are normally not significant due to interspecies variability. Among the animal models, porcine lumbar intervertebral discs (PLIVD) are considered as an accepted model for mechanical testing of the spine, as they present both functional and anatomical similarities with human ones [29], [33]. However, there is a lack of information about the differences between the mechanical properties of PLIVD and human lumbar intervertebral discs (HLIVDs) [29].

Thus, the first aim of this work is to quantify the mechanical properties of PLIVD under quasi-static and cyclic axial compressive loading. Consequently the K_s and K_d of PLIVDs will be experimentally determined and compared. The acquired values will be also correlated with those reported on literature for HLIVDs, to check if PLIVDs are a good model to study the mechanical properties of human samples under compression.

In addition, to numerically describe the viscoelastic behavior of IVDs, several rheological mathematical models were used [14], [16], [19], [25], [28]. The formulation adopted to model the creep behavior of the disc results from the combination of parallel springs and dashpots sets (viscoelastic solid Voigt model) with a spring in serial, representing the initial elastic behavior [14], [16], [19], [25], [28]. These mathematical models are very useful since they allow the state prediction of the IVD after a certain time [25], being also used to test differences between study groups, such as comparing the behavior of human and animal samples.

As second goal, this work proposes to compare the model parameters obtained for the PLIVD with the values reported on literature for the HLIVD. To achieve it, a phenomenological model [25] was used to fit on experimental creep data for PLIVDs. This study considered that the adjacent vertebral bodies are uncompressible, for the range of loads applied. Consequently, the IVD is the only structure subjected to deformation on the MS.

In this study, the optimized set of model parameters was determined and compared with those found in literature, for HLIVDs. The premise is that the parameters values may help understanding the differences between the HLIVDs and PLIVD behavior.

2. Materials and methods

2.1. MS collection and preparation

Two porcine lumbar spines, from young cadavers (with approximately eighteen months), were collected from an abattoir. Motion segments (IVD and half of both the adjacent vertebral bodies, without posterior elements) were cut from the spines, parallel to the mid-transverse plane of the disc. In addition, all specimens were visually inspected before and immediately after the mechanical test. Care was taken to remove the surrounded tissues during dissection. The segments were stored at 4 °C before testing, which were performed within 24 h after dissection, in accordance with a protocol approved by the Institutional Human Tissue Committee [5].

The specimens were immersed in a phosphate saline solution (PBS 1X) before, during and after the mechanical test, to prevent the dehydration. The degeneration grade was assessed by Thompson five-category grading scheme [32], after testing. All discs presented a level I on Thompson degeneration scale.

2.2. Testing equipment and MS positioning

The testing equipment consists of a servo hydraulic testing system, Instron 8874, with both quasi-static

and dynamic loading modes, equipped with a 2500 kN load cell. The samples were placed on compression grips and aligned to minimize the effects of bending/extension that could occur on a compression test with a misaligned sample. Thus, the samples were positioned in a center of a cast aluminum pot, parallel to the base. This pot was filled with PBS (1X), to keep the samples entirely submerged. All tests were carried out at room temperature.

2.3. Quasi-static axial compressive test

During quasi-static axial compressive tests, the samples (n = 7) were first submitted to a pre-load of 30 N, during 10 minutes, to ensure the contact with loading platen, helping to minimize errors due to post-mortem effects, such as the super hydration [5]. Then, load and displacement was set to zero and each sample was submitted to 50 N load (Phase 1). Then, the displacement reached for 50 N load was maintained during 7.5 min and, subsequently, the samples were loaded until reach 500 N (Phase 2). This kind of loading was applied in order to understand the effect of loading magnitudes on the Ks of lumbar porcine IVDs. In this work, we adopted a range of loading considered as an appropriate estimation for the PLIVDs axial loading experienced in daily life [29]. A generic example of the quasi-static axial compressive test input is shown in Fig. 2.

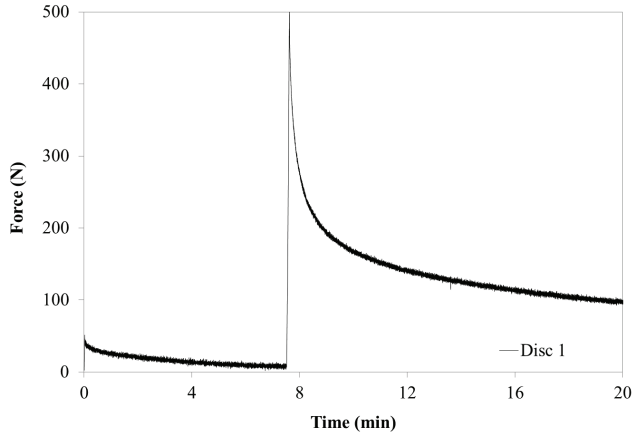

Fig. 2. A generic example of the quasi-static axial compressive test input, used for the disc 1. After pre-load application, load and deformation were set to zero and each sample was submitted to 50 N load. The displacement reached at 50 N is kept during 7.5 min. Consequently, the samples were loaded with 500 N (n = 7), at different strain rates (4 and 16 mm/min). Finally, the displacement, reached at 500 N, is kept during 12 minutes

In addition, the displacement rates were set to 4 mm/min and 16 mm/min, which correspond to the physiological load rates, experimented by a human when submitted to an inclination of 30 degrees and when a human is getting up, respectively. The displacement rates were determined from the curves presented on the database OrthoLoad [2], from which the slope of the curves force as function of time, for these movements, was converted into displacement rates.

The displacement rates used on this work are considered as quasi-static. Thus, the static stiffness coefficient, K_s, was defined as the slope of each loading increment (from both 0–50 N and 50-500 N increments), being determined using a linear trend on the load-displacement curve.

In terms of statistical analysis, the four groups of K_s values (phase 1 at 4 mm/min; phase 1 at 16 mm/min; phase 2 at 4 mm/min and phase 2 at 16 mm/min) were compared by a 2-factor ANOVA. According to this analysis, a t-test with two-sample was used to characterize the significant differences between each phase and displacement rate. All statistical analyses were performed with Microsoft Excel® and significance level $p < 0.05$.

2.4. Cyclic compressive tests

An initial 30 N compressive load was applied, in order to ensure the contact loading platen. Each MS (n = 5) was subjected to 1200 cycles of axial compressive loading, at a frequency of 1 Hz. The mean load was 500 N, with amplitude of 125 N.

The data from cyclic load phase was used to determine the dynamic stiffness coefficient K_d, which was calculated dividing the peak-to-peak load applied by the peak-to-peak displacement, for each loading cycle [19]. The final K_d value in this study was determined by the arithmetic mean of dynamic stiffness coefficient, obtained for each cycle.

2.5. Five-parameter rheological model for creep response analysis

To compare the creep behaviour of LPIVD with HPIVD, the experimental data were fitted into a phenomenological model, using equation (1), developed by O'Connell [25]. This model allows the prediction of the displacement that occurs on human IVDs, as a function of time. It consists on a five-parameter rheological model, composed by two Voigt solids and a spring in series and it is used to determine the displacement (d, in millimetres), as a function of time (t, in seconds) and applied load (L, in newtons). The model is mathematically described as

$$d(t = t_i \rightarrow t_{i+1}) = L \times \left[\left(\frac{1}{S_1} \left(1 - c^{-\frac{t}{\tau_2}} \right) \right) + \left(\frac{1}{S_2} \left(1 - c^{-\frac{t}{\tau_2}} \right) + \frac{1}{S_E} \right) \right] \quad (1)$$

where S_1 and τ_1 are related to the fast response, S_2 and τ_2 to the slow response, and S_E the elastic response. In addition, i and $i + 1$ represent the start and the end time for the creep test.

The experimental data were filtered and the displacement-time curve was traced considering the average displacement for each compression cycle. The objective was to minimize the noise resulting from a cyclic curve. A mean force of 500 N was adopted as the L value. The minimization of the sum of the squared error between the predicted and the experimental displacement during creep test allows the determination of the constants of the 5-parameter model for the IVDs. The parameters acquired experimentally were compared directly with reported literature for human samples.

3. Results

Previous studies showed that IVDs from the lumbar zone present a non-linear load-deflection curve in quasi-static conditions [11]. However, in this study the K_s values were obtained from a linear regression with $R^2 > 0.92$ (Fig. 3), indicating this approach presents a good fit for the experimental data.

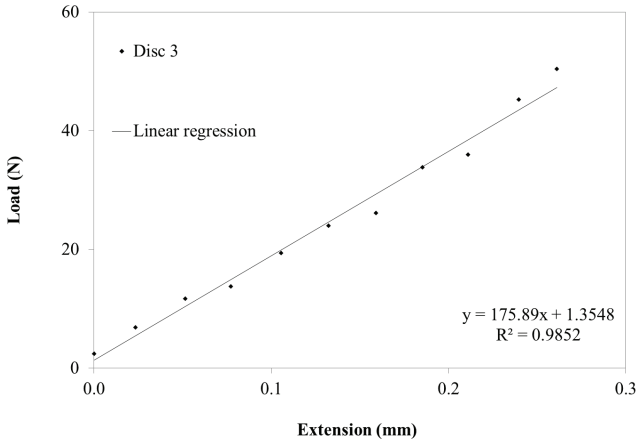

Fig. 3. A linear regression performed on a MS sample, at a load rate of 16 mm/min, for a 0–50 N increment. The slope of this regression represents the static stiffness coefficient, K_s, which is defined as the slope of each loading increment (from both 0–50 N and 50–500 N increments)

In this study, for the first slope (0 until 50 N), the values of stiffness coefficient were lower 0.485 ± 0.127 MN/m (mean ± SD) than those found on load slope (until 500 N), where the K_s is 1.215 ± 0.248 MN/m (Fig. 4). The ANOVA test showed that there are significant differences between the mean values of the data groups analysed. Then, the t-test revealed that there are significant differences on K_s according to the magnitude of the load applied (between phase 1 at 4 mm/min and phase 2 at 4 mm/min; between phase 1 at 16 mm/min and phase 2 at 16 mm/min; $p < 0.05$), while non-significant differences were found when different displacement rates were applied (between phase 1 at 4 mm/min and phase 1 at 16 mm/min; between phase 2 at 4 mm/min and phase 2 at 16 mm/min; $p < 0.05$).

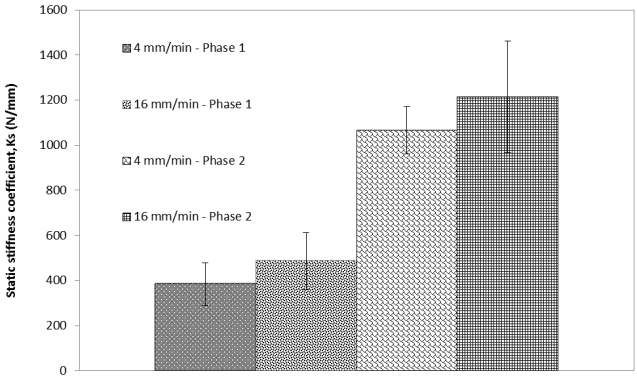

Fig. 4. Bar chart representing the K_s for two different strain rates: 4 mm/min and 16 mm/min. Two different phases were also distinguished: phase 1 represents the K_s for increasing from 0 until the pre-load (50 N), while phase 2 represents the increasing of load until reaching 500 N, for the two strain rates

In terms of K_d, the results (Table 1) indicated an oscillation of the K_d between specimens, for five IVDs. The comparison of the K_d results with those obtained in a previous study for human IVDs [19] (Table 1), revealed that K_d is, at least, two times higher than the values presented for human samples. In addition, the magnitude of K_d values is between four and ten times higher than those obtained for K_s, depending on load applied.

Table 1. Experimental dynamic stiffness coefficient (K_d), obtained in this study PLIVDs ($n = 5$; mean and standard deviation), and HLIVDs K_d (mean) found in a previous study performed by Li et al. [19], at 1 Hz

	Li et al. [19]	This study
K_d (MN/m)	2.42 ± 0.51	5.41 ± 0.05

The five-parameter model presented an average relative error of 0.2% for the fitting to the experimental data (Fig. 5). Thus, the rheological model presented a good fit for the set of parameters found during this study (Table 2).

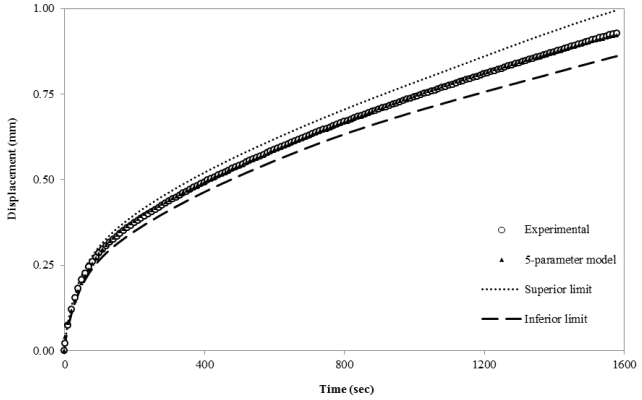

Fig. 5. A comparison between the creep responses of the experimental obtained with PLIVD and the five parameter rheological model. The values were fit by the inferior and superior limits, with a confidence interval of 95%

Table 2. Comparison between model parameters obtained with the best fit to the experimental results with PLIVDs (mean, inferior and superior limit with a confidence interval of 95%) and the values obtained by O'Connell et al. [25] for HLIVDs (mean and interquartile range)

	Present study	O'Connell et al. [25]
τ_1 (min)	32.04 (23.23, 47.13)	8.09 (6.12, 11.75)
L/S_1 (mm)	1.16 (0.91, 1.61)	0.29 (0.21, 0.44)
τ_2 (h)	0.18 (0.17, 0.31)	3.07 (2.96, 3.43)
L/S_2 (mm)	0.27 (0.23, 0.31)	1.51 (1.31, 1.72)
L/S_E (mm)	0.016 (0.016, 0.016)	1.44 (1.08, 1.71)

The time constants are approximately four times higher (in the case of τ_1) and seventeen times lower (for τ_2) than those found by O'Connell et al. [25]. The porcine displacement parameters L/S_2 and L/S_E (that correspond to slow displacement and elastic displacement, respectively) presented lower values than those obtained for human IVDs (L/S_2 is six times lower and L/S_E is around ninety times). Contrarily, L/S_1, which is a parameter of fast response, is around four times higher than previous values [25].

4. Discussion

In this study, the mechanical properties of PLIVD were evaluated under quasi-static and dynamic conditions and the obtained data were compared with published values for HLIVD. Moreover, the experimental data were fitted into a phenomenological model (equation (1)), developed by O'Connell et al. [25]. The results documented in this paper lead to important considerations, in both quasi-static and dynamic conditions.

A linear regression was used to calculate the K_s, with a minimum R^2 of 0.92, indicating a good fit to experimental data.

However, the values of K_s are lower for PLIVDs than for human samples (Table 3), which can be explained by the fact of PLIVDs in this study derived from young animal specimens and so, it is expected that they behave more elastically and less stiffly than the human samples used in the previous studies. Since the load was applied on fresh thawed lumbar spines, the K_s magnitude should be significantly lower for smaller loads. Thus, a lower value of K_s for Phase 1 (0–50 N load) is an expectable value. In addition, a higher value of K_s was obtained on this PLIVD during the application of the second loading phase (from 50 N to 500N), since this is stiffer than the first loading phase (from 0 to 50 N).

Table 3. Comparison between K_s and the maximum load applied to HLIVD (obtained in previous studies) and PLIVD (this study)

Authors	K_s (MN/m)	Maximum load (N)
Virgin [34]	2.5	4500
Hirsch and Nachemson [10]	0.7	1000
Brown et al. [3]	0.1–1.5 (initial slope) 2.1–3.6 (major slope)	450–900
Markolf and Morris [23]	1.23–3.32 (tangent at max. load)	220–670
Asano et al. [1]	0.49 (0.04) (0–0.5 mm) 0.73 (0.06) (0.5–1 mm) 1.18 (0.09) (1–1.5 mm)	1500
Izambert et al. [11]	0.05 (0.02) (until 0.5 mm) 0.64 (0.1) (until 1.5 mm) 0.60–0.94 (tangent at max. load)	400
Present study	0.49 (0.13) (until 0.5 mm – 50 N) 1.215 (0.248) (from 0.5 mm – 50 N – until 1.5 mm – 500 N)	500

These data are confirmed by earlier studies (Table 3), where it is reported that K_s presents a high dependence on load or displacement imposed on the specimen. This phenomena is even more evident by the highest value for K_s documented for human IVDs [34], which is not mechanically representative, since 4.5 kN is above the maximum physiological values (forces that did not induce irreversible deformation on discs) for humans [6]. For the first slope (until 0.5 mm of displacement and 50 N of load), the values present the

same magnitude of those found by Asano et al. [1]; the results for phase 2 (slope until reaching 500 N) are also close to those found in literature, namely for those obtained for Markolf and Morris [23] and Asano et al. [1]. These data indicate that the magnitude of load applied and the method of stiffness calculation [11] are likely the causes for the divergence found between human data in Table 3.

No difference was detected in the magnitude of K_s found in human and porcine samples, for both load-displacement slopes, indicating that PLIVD can be useful for the determination of quasi-static behaviour of HLIVD. Moreover, the values of K_s of the IVDs did not reveal significant differences for different physiological displacement rates, meaning that changes in displacement rate, during the daily routine movements, do not have an important effect on the K_s of PLIVDs.

It is important to note that several options could be considered for the calculation of the elastic stiffness response of the IVD, since it presents an elastoplastic behavior, i.e., some of the mechanical work (or energy) is irreversibly dissipated into heat, in a way that it can never be recovered as such again [20]. However, in this study, the K_s was calculated using a simplified approach referenced in literature [25]: the slope of the linear-region of the force-displacement curve.

The comparison of the K_d results with those obtained in previous study for HLIVDs [19] showed that porcine K_d is two times higher than the human one. Furthermore, the K_d is between four and ten times higher than K_s, which is in opposition to what is referred to in literature, where K_d and K_s appear to present the same range of values, for low frequencies [11]. The differences between these results and the literature could be justified by the choice of the viscoelastic model (which affects the mode of K_d calculation [11]) and the different experimental setups adopted [15]. Here, the K_d calculation came directly from experimental data, without any model manipulation. In addition, this work revealed a short variation (SD) when compared to the data exposed by Li et al. [19]. Since the samples were originating from different porcine lumbar motion segments of the same specimen, this could indicate that there is a minimal K_d difference for different intra-specimen PLIVDs samples.

Concerning the IVD fluid flow and transport, it represents a complex three-dimensional problem, evolving several questions such as the strain-dependent permeability, anisotropy and inhomogeneity [6]. Thus, although the use of sophisticated models to understand the mechanisms of IVD flow and transport under load [7], [22], this process remains still unclear. Consequently, the development of optimized constitutive models and experiments is essential in order to better understand the process of fluid flow.

However, the viscoelastic models can be used as simplified tool to understand the mechanics of fluid flow on the IVD [14], [25], [28]. These models provide parameters that can be useful to describe the time-dependent mechanics and the viscoelasticity of IVD, as well as to identify the fluid flow differences between animal and human IVDs [14], [16], [19], [28].

For the parameters of the viscoelastic model adopted in this study (Table 2), the authors associated the differences in time constants τ_1 and τ_2 to the changes in the fluid flow pathway, while the displacement amplitude constants (L/S_1, L/S_2 and L/S_E) were related to the quantity of fluid exchange in that pathway [25]. The difference between human and porcine time constants are likely linked to the influence of fluid flow pathway and strain-dependent permeability [13], [33]. Previous studies proposed that parameters of fast response (τ_1 and L/S_1) are more connected to the fluid flow through NP or endplate, and the slow response, τ_2 and L/S_2, is more related to AF fluid flow [13], [25].

Earlier studies also showed that τ_1 increases with nucleotomy, in a compressive cyclic loading [13], resulting in both a lower NP and endplate permeability. However, it is also known that NP presents an increased permeability with severe degeneration, resulting in an easier and faster flow [12]. Therefore, the higher porcine τ_1 is presumably caused by a lower NP and endplate permeability, which could be explained by the age and condition of PLIVDs used in this study: they were taken from young animals and were not frozen, allowing keeping a good physiological condition of IVD, in a non-degenerated state. In addition, while test executed by O'Connell et al. [25] was performed during 5 hours, the present experiment took around half hour. Thus, the poroelastic response, which is normally a slow response event, was minimized [6]. Consequently, the parameters of slow response reported in this work are not relevant, since their effect is only visible in the magnitude of hours.

The displacement parameters L/S_2 and L/S_E, which correspond to slow displacement and elastic displacement, respectively, indicate that the volume and distance of fluid flowing on the pathway is likely higher during the fast response and lower for slow response. This is expectable, since this study is focused on the fast response due to the short time of test applied on IVD, being predictable that the fluid flow occurs predominantly during the fast response.

Although during the fast response the NP and endplate present low permeability, the major displacement due to fluid flow occurs during this phase. This suggests that after the load application, even though the AF fluid outflow normally occurs during slow response, in the case of PLIVDs it may also occur during fast response, overwhelming the low permeability of NP and endplate. This is supported by Ellingson and Nuckley [9], who noticed that AF has a significant role in the IVD's fast response, whereas the NP may have a minor intervention during this phase.

Even though the load has been normalized by the viscoelastic model, these assumptions can be influenced by the magnitude of the load applied. Previous studies had reported that 1000 N load on human IVD samples (used by O'Connell et al. [25]) correspond to a load limit of the IVD [6], which is a force magnitude that could lead to a dramatic change in the osmotic pressure of IVD, promoting a quick expel of the fluid out of the system [31]. In this study, 500 N of creep load was applied, which corresponds, even in PLIVDs, to a loading range (0–800 N) considered as an appropriate estimation for the axial loading experienced in daily life [29].

There are obviously many aspects to consider when an animal model is chosen, and these differences must be considered in both experimental design and data interpretation [8]. However, the existence of striking similarities between the spines of human and quadrupeds is unarguable: the quadruped spine is essentially loaded in the same way as that of a human [30]; in addition, the curvature of the spine does not influence the way a motion segment or an intervertebral disc is loaded [26]. In the particular case of the lumbar porcine models, they are readily available and not subject to stringent regulations. Moreover, the morphometric data for both porcine vertebrae and disc are described in detail, helping the researchers to choose the most appropriate experimental procedure [4], [28]. All of these facts help to justify the use of these animals as model for the study of human spine behavior.

Moreover, the viscoelastic model applied can be considered as simplification of a complex mechanical and physiological process, bringing important parameters to better understand the fluid flowing in IVD. This model presents an excellent agreement between experimental and predicted displacements, showing that it is well suited to analyze the creep of an entire motion segment. However, it presented some limitations, including the fact that the parameters of the simple viscoelastic model did not represent invariant material properties since they could vary with testing conditions [28]. Still, this model showed that care must be taken in the direct mechanical behaviour comparison between PLIVDs and HLIVD: they present different anatomical and physiological properties [29], as well as relevant differences in terms of quasi-static and dynamic response.

Concluding, although the complex poroelastic flow under load is not totally understood, this model confirmed that several phenomena govern the fluid flow in the IVD. Thus, the present model could act as an important tool to understand the differences between PLIVD and HLIVD behaviour.

Future works should be focused on the long term effect of the IVD hydration and the influence of the ligaments on the response of motion segment to quasi-static and dynamic load. In addition, techniques as ultrasonic tests [17] or quasi-static unloading experiments [20] had revealed to be promising and must be considered in capturing the "truly" elastic behavior of IVD.

Acknowledgements

This work was funded by the project "NP Mimetic–Biomimetic Nano-Fibre Based Nucleus Pulposus Regeneration for the Treatment of Degenerative Disc Disease", financed by the European Commission under FP7 (grant NMP-2009-SMALL-3-CP-FP 246351).

The authors also express their gratitude to Indústria de Carnes do Minho (ICM) – Primor Group – for the possibility of collecting spine column samples in their facilities.

References

[1] ASANO S., KANEDA K., UMEHARA S., TADANO S., *The mechanical properties of the human L4-5 functional spinal unit during cyclic loading. The structural effects of the posterior elements*, Spine, 1992, Vol. 17, 1343–1352.

[2] BERGMANN G. (ed.), *Charité Universitaetsmedizin Berlin*, "OrthoLoad", 2008.

[3] BROWN T., ROBERT H.J., YORRA A.J., *Some Mechanical Tests on the Lumbosacral Spine with Particular Reference to the Intervertebral Discs*, J. Bone Joint. Surg. Am, 1957, Vol. 39-A, 1135–1164.

[4] BUSSCHER I., PLOEGMAKERS J.J.W., VERKERKE G.J., VELDHUIZEN A.G., *Comparative anatomical dimensions of the complete human and porcine spine*, Eur. Spine J., 2010, Vol. 19, 1104–1114.

[5] CAMPBELL-KYUREGHYAN N.H., YALLA S.V., VOOR M., BURNETT D., *Effect of orientation on measured failure strengths of thoracic and lumbar spine segments*, J. Mech. Behav. Biomed. Mater., 2011, Vol. 4, 549–557.

[6] CASTRO A.P.G., *Development of a biomimetic finite element model of the intervertebral disc diseases and regeneration*, Dissertation, University of Minho, 2014.

[7] CASTRO A.P.G., WILSON W., HUYGHE J.M., ITO K., ALVES J.L., *Intervertebral disc creep behavior assessment through an open source finite element solver*, J. Biomech., 2014, Vol. 47, 297–301.

[8] DATH R., EBINESAN A.D., PORTER K.M., MILES A.W., *Anatomical measurements of porcine lumbar vertebrae*, Clin. Biomech., 2007, Vol. 22, 607–613.

[9] ELLINGSON A.M., NUCKLEY D.J., *Intervertebral disc viscoelastic parameters and residual mechanics spatially quantified using a hybrid confined/in situ indentation method*, J. Biomech., 2012, Vol. 45, 491–496.

[10] HIRSCH C., NACHEMSON A., *New observations on the mechanical behavior of lumbar discs*, Acta Orthop. Scan., 1954, Vol. 23, 254–283.

[11] IZAMBERT O., MITTON D., THOUROT M., LAVASTE F., *Dynamic stiffness and damping of human intervertebral disc using axial oscillatory displacement under a free mass system*, Eur. Spine J., 2003, Vol. 12, 562–566.

[12] JOHANNESSEN W., ELLIOTT D.M., *Effects of degeneration on the biphasic material properties of human nucleus pulposus in confined compression*, Spine, 2005, Vol. 30, 724–729.

[13] JOHANNESSEN W., VRESILOVIC E.J., WRIGHT A.C., ELLIOTT D.M., *Disc mechanics with trans-endplate partial nucleotomy are not fully restored following cyclic compressive loading and unloaded recovery*, J. Biomech. Eng., 2006, Vol. 128, 823–829.

[14] JOHANNESSEN W., VRESILOVIC E.J., WRIGHT A.C., ELLIOTT D.M., *Intervertebral disc mechanics are restored following cyclic loading and unloaded recovery*, Ann. Biomed. Eng., 2004, Vol. 32, 70–76.

[15] KASRA M., SHIRAZI-ADL A., DROUIN G., *Dynamics of human lumbar intervertebral joints. Experimental and finite-element investigations*, Spine, 1992, Vol. 17, 93–102 .

[16] KELLER T.S., SPENGLER D.M., HANSSON T.H., *Mechanical behavior of the human lumbar spine. I. Creep analysis during static compressive loading*, J. Orthop. Res., 1987, Vol. 5, 467–478.

[17] KOHLHAUSER C., HELLMICH C., VITALE-BROVARONE C., BOCCACCINI A.R., ROTA A., EBERHARDSTEINER J., *Ultrasonic Characterisation of Porous Biomaterials Across Different Frequencies*, Strain, 2009, Vol. 45, 34–44.

[18] KORECKI C.L., MACLEAN J.J., IATRIDIS J.C., *Dynamic compression effects on intervertebral disc mechanics and biology*, Spine, 2008, Vol. 33, 1403–1409.

[19] LI S., PATWARDHAN A.G., AMIROUCHE F.M., HAVEY R., MEADE K.P., *Limitations of the standard linear solid model of intervertebral discs subject to prolonged loading and low-frequency vibration in axial compression*, J. Biomech., 1995, Vol. 28, 779–790.

[20] LUCZYNSKI K.W., BRYNK T., OSTROWSKA B., SWIESZKOWSKI W., REIHSNER R., HELLMICH C., *Consistent quasistatic and acoustic elasticity determination of poly-L-lactide-based rapid-prototyped tissue engineering scaffolds*, J. Biomed. Mater Res., Part A, 2013, vol. 101, 138–144.

[21] MACLEAN J.J., OWEN J.P., IATRIDIS J.C., *Role of endplates in contributing to compression behaviors of motion segments and intervertebral discs*, J. Biomech., 2007, Vol. 40, 55–63.

[22] MALANDRINO A., NOAILLY J., LACROIX D., *The effect of sustained compression on oxygen metabolic transport in the intervertebral disc decreases with degenerative changes*, PLoS Comput. Biol., 2011, Vol. 7, e1002112.

[23] MARKOLF K.L., MORRIS J.M., *The structural components of the intervertebral disc. A study of their contributions to the ability of the disc to withstand compressive forces*, J. Bone Joint. Surg. Am., 1974, Vol. 56, 675–687.

[24] MASUOKA K., MICHALEK A.J., MACLEAN J.J., STOKES I.A.F., IATRIDIS J.C., *Different effects of static versus cyclic compressive loading on rat intervertebral disc height and water loss in vitro*, Spine, 2007, Vol. 32, 1974–1979.

[25] O'CONNELL G.D., JACOBS N.T., SEN S., VRESILOVIC E.J., ELLIOTT D.M., *Axial creep loading and unloaded recovery of the human intervertebral disc and the effect of degeneration*, J. Mech. Behav. Biomed. Mater., 2011, 4, 933–942.

[26] PATWARDHAN A.G., HAVEY R.M., MEADE K.P., LEE B., DUNLAP B., *A Follower Load Increases the Load-Carrying Capacity of the Lumbar Spine in Compression*, Spine, 1999, Vol. 24, 1003-1009.

[27] PÉRIÉ D., KORDA D., IATRIDIS J.C., *Confined compression experiments on bovine nucleus pulposus and annulus fibrosus: sensitivity of the experiment in the determination of compressive modulus and hydraulic permeability*, J. Biomech., 2005, Vol. 38, 2164–2171.

[28] POLLINTINE P., VAN TUNEN M.S.L.M., LUO J., BROWN M.D., DOLAN P., ADAMS M.A., *Time-dependent compressive deformation of the ageing spine: relevance to spinal stenosis*, Spine, 2010, Vol. 35, 386–394.

[29] RYAN G., PANDIT A., APATSIDIS D., *Stress distribution in the intervertebral disc correlates with strength distribution in subdiscal trabecular bone in the porcine lumbar spine*, Clin. Biomech., 2008, Vol. 23, 859–869.

[30] SMIT T.H. *The use of a quadruped as an in vivo model for the study of the spine – biomechanical considerations*, Eur. Spine J., 2002, Vol. 11, 137–144.

[31] STOKES I.F., LAIBLE J.P., GARDNER-MORSE M.G., COSTI J.J., IATRIDIS J.C., *Refinement of elastic, poroelastic, and osmotic tissue properties of intervertebral disks to analyze behavior in compression*, Ann. Biomed. Eng., 2011, Vol. 39, 122–131.

[32] THOMPSON J.P., PEARCE R.H., SCHECHTER M.T., ADAMS M.E., TSANG I.K., BISHOP P.B., *Preliminary evaluation of a scheme for grading the gross morphology of the human intervertebral disc*, Spine, 1990, Vol. 15, 411–415.

[33] VAN DER VEEN A.J., MULLENDER M.G., KINGMA I., VAN DIEEN J.H., VAN J.H., SMIT T.H., *Contribution of vertebral [corrected] bodies, endplates, and intervertebral discs to the compression creep of spinal motion segments*, J. Biomech., 2008, Vol. 41, 1260–1268.

[34] VIRGIN W.J., *Experimental properties into the physical properties on the intervertebral disc*, J. Bone Joint. Surg., 1951, Vol. 33, B.

[35] ZHANG Y., DRAPEAU S., AN H.S., MARKOVA D., LENART B.A., ANDERSON D.G., *Histological features of the degenerating intervertebral disc in a goat disc-injury model*, Spine, 2011, Vol. 36, 1519–1527.